HOKKAIDO UNIVERSITY

Title	Torsional Stress Analysis for a Continuous Box Girder Bridge with a Variable Cross Section and its Numerical Examples
Author(s)	Saeki, Noboru; Fujita, Yoshio
Citation	, 68(1), 91-104
Issue Date	1973-09-25
Doc URL	http://hdl.handle.net/2115/41147
Type	bulletin (article)
File Information	68(1)_91-104.pdf

Torsional Stress Analysis for a Continuous Box Girder Bridge With a Variable Cross Section and its Numerical Examples

Noboru SAEKI and Yoshio FUJITA*

(Received March 23, 1973)

Abstract

Torsion-bending theory in consideration of deformation due to secondary shearing stress is proposed by the authors and torsional stress on a continuous beam with varible cross sections is analyzed by the theory. Results of model beam test on a box-beam having a length of 50 cm, a width of 4 cm and a height of 3 cm, are compared with values calculated by Bornscheuer's, Grasse's and the author's theory, and it was ascertained that the proposed theory in the present paper has a higher degree of accuracy as compared with the others.

Influence lines of primary torsional moment, secondary torsional moment, warping moment, and torsional stress are calculated by this theory and compared with Bred't and Bornscheuer's, thus it was clarified that the torsional stress on continuous concrete beams takes an intermediate value between Bredt's and Bornscheuer's.

1. Introduction

In construction of a concrete girder bridge with a long span, a type of statically indeterminate box girder with variable crosss sctions has been widely used and owing to the progress of quality of materials and execution of work, thin-walled box beams have come into use and dead load has been lightened. Therefore it has become possible to design a bridge with longer span. In this paper the problem of a torsional stress continuous beam with thin-walled box is discussed on the base of torsion-bending in consideration of deformation due to secondary shearing stress. Torsional stresses on fixed beam and simple-fixed beam have been reported in the previous paper[1].

Formerly, the torsion-bending theory was established by Wagner[2] and systematically described by Bornscheuer[3] and Vlasov[4].

Recently the theory in consideration of the deformation due to secondary shearing stress has been presented by Heilig[5], Roik[6] and Grasse[7].

In these papers the deformation due to secondary shearing flow was assumed in the same direction, thus these theories were generally tend to estimate excessive deformation.

In this paper the secondary deformation is given by the way of "the principle of virtual work", taking into account the direction of the secondary shear flow, thus the deformation has a tendency to be smaller than Heilig's and Grasse's. In order to clarify the differences among the theories by Heilig, Grasse and the author,

---

* 土木工学部 交通構造工学講座

numerical examples are shown in the figures concerning coefficients indicating the effect of deformation due to secondary shearing stress, and further, model beams made of acrylic resin is experimentally tested to verify the theory of torsion-bending in consideration of the secondary deformation. Internal forces of a continuous beam with variable cross section are analyzed by "Knoten Last" method and influence lines of m_t, $\bar{m}_t$, and m_w and torsional stress are discusssed.
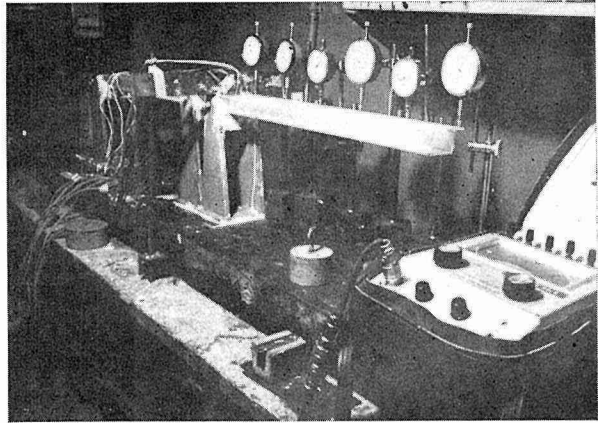
Picture 1   Model test beam

2.   Notation

$T =$ total torsional moment

$m_t =$ primary torsional moment

$\bar{m}_t =$ secondary torsional moment

$m_w =$ warping moment

$\theta =$ angle of rotation

$\theta_s =$ angle of rotation of Saint-venant's part

$V_s =$ displacement in s-direction

$W =$ displacement in z-direction

$s =$ curvilinear coordinate

$\sigma =$ warping stress

$\tau =$ primary shearing stress

$\bar{\tau} =$ secondary shearing stress

$\gamma =$ primary shearing strain

$\bar{\gamma} =$ secondary shearing strain

$\gamma^* =$ total shearing strain

$q_s =$ primary shear flow

$\bar{q} =$ secondary shear flow

$D =$ shear center

$r_D =$ radius from shear center

$F =$ area enclosed by the center line of the cross section

$EC_w =$ sectorial rigidity

$GI_t =$ torsional rigidity

$I_B =$ torsion constant by Bredt

$I_s =$ torsion constant by Saint-venant

$I_c =$ torsion constant calculated by Trefftz's method

3.　Assumption

(a)　Preservation of the shape of the cross section.

This means that the function $V_s(s, z)$ and $\theta(s, z)$ must be constant in all points of the cross section, namely

Fig. 1.　Coordinate system

$$V_s = V_s(z), \qquad \theta = \theta(z)$$

(b)　Propotion between stresses and strains.

The material satisfies Hooke's law.

$$\sigma = E \frac{\partial W}{\partial z}$$

(c)　Thin-walled cross section

It is necessary that primary shear flow be constant in all points of closed cross section.

In order to verify the validity of the assumption "Thin-walled", numerical example is calculated by Trefftz's[8] method as shown in Table 1 and Fig. 2. It was noted that the slope of the curves I_c/I_B are very small in the range of the ratio of $t/h < 0.2$, therefore within that range the primary shear flow is almost uniform.
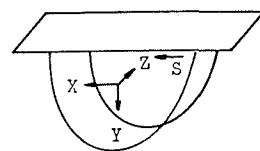
Table 1.

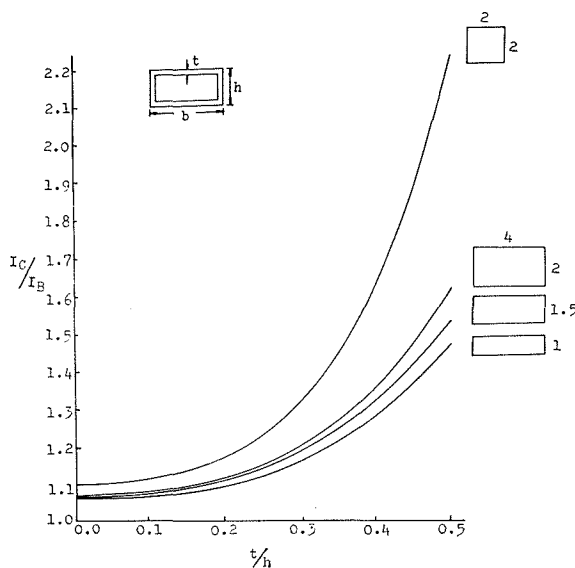| $b \times h \times t$ (m)	I_c	I_B	$I_c/I_B + I_s$	$b \times h$ (m)	I_c	I_s
$2 \times 2 \times 0.4$	1.918	1.638	1.071	2×2	2.244	2.249
$4 \times 2 \times 0.4$	5.795	5.104	1.085	4×2	7.318	7.320
$4 \times 1.5 \times 0.4$	3.085	2.667	1.070	4×1.5	3.437	3.428
$4 \times 1.0 \times 0.2$	0.880	0.804	1.063	4×1.0	1.124	1.131

Fig. 2.

3.1   Torsion-Bending Theory in Consideration of the Deformation due to Secondary Shearing Stress

We obtained primary shearing strain γ_s due to primary shear flow q_s as shown in Fig. 3,

$$\gamma_s = \frac{\partial V_s}{\partial z} + \frac{\partial W}{\partial s} = \frac{q_s}{Gt} \qquad (1)$$

Fig. 3.   Deformation of an element

Secondary shear strain $\bar{\gamma}$ due to secondary shear flow $\bar{q}$ is shown by a dotted line in Fig. 3 and we obtain the folloing,

$$\bar{\gamma} = \frac{\partial \overline{V}}{\partial z} \qquad (2)$$

Displacement V_s due to rotation of θ_s is

$$V_s = r_D \cdot \theta_s \qquad (3)$$

Substituting these into Eq. (1) and preforming the integration in regard to W, we find

$$W = \theta'_s \int r_D ds + \frac{1}{G} \int q_s \frac{ds}{t} + W_0 \qquad (4)$$

where W_0 is a constant of integration.

The longitudinal deformation W is defined as follows

$$W = \varphi \theta'_s \qquad (5)$$

where

$$\varphi = -\int r_D ds + \frac{1}{G\theta'_s} \int q_s \frac{ds}{t} + \varphi_0 \qquad (6)$$

φ is called warping function. φ_0 is a constant of integration. The continuity condition

$$\int \frac{\partial \varphi}{\partial s} ds = 0$$

must be satisfied, substituting Eq. (6) into the above condition. We obtain

$$\frac{q_s}{G\theta'_s} = \frac{2F}{\oint \frac{ds}{t}} \qquad (7)$$

Substituting this in Eq. (6), we find

$$\varphi = -\int r_D ds + \frac{2F}{\oint \frac{ds}{t}} \int \frac{ds}{t} + \varphi_0 \qquad (8)$$

Warping stress and secondary shearing stress acting at an element are shown in Fig. 4. The equilibrium condition of the element in the longitudinal direction is represented as follows

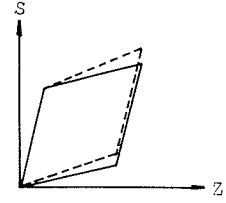$$\frac{\partial \sigma t}{\partial z} + \frac{\partial \bar{q}}{\partial s} = 0 \qquad (9)$$
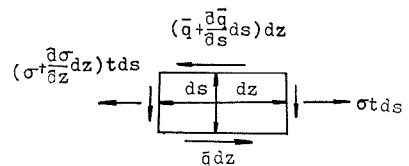
Fig. 4.   Stresses acting at an element

By performing the integration.

$$\bar{q} = q_0 - \int \sigma' t \, ds \qquad (10)$$

where q_0 is a constant of integration.

The strains are related with the stresses by Hooke's law as follows.

$$\sigma = E \frac{\partial W}{\partial z} = E\varphi\theta_s'' \qquad (11)$$

Substituting this into Eq. (10).

$$\bar{q} = q_0 - E\theta_s'' F_\varphi \qquad (12)$$
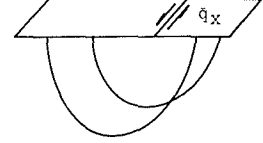
where

$$F_\varphi = \int \varphi dF$$

Fig. 5. Redundant force

The continuity condition of the strain produced by secondary shear flow, that is $\Delta W = 0$, must be satisfied.

By applying "the principle of virtual work", as shown in Fig. 5, we obtain

$$\Delta W = \int \tau \bar{r} \, dV = \frac{1}{G} \oint (\bar{q}_0 - E\theta_s'' F_\varphi) \frac{ds}{t} = 0 \qquad (13)$$

$\bar{q}_0 / E\theta_s'''$ is denoted $\bar{q}_x$, and we find

$$\bar{q}_x = \int F_\varphi \frac{ds}{t} \bigg/ \oint \frac{ds}{t} \qquad (14)$$

Substituting this in Eq. (12)

$$\bar{q} = -E\theta_s'''(F_\varphi - \bar{q}_x) \qquad (15)$$

Distribution of the secondary shear flow $\bar{q}$ has a parabolic form and the additional unit rotation $\bar{\theta}'$ yields due to the shear flow $\bar{q}$.

Displacement in the direction of s by the angle of rotation $\bar{\theta}$ is related as follows.

$$\overline{V} = r_D \bar{\theta} \qquad (16)$$

From Eq. (1) and Eq. (2), total shearing strain r^* is

$$r^* = \frac{\partial V_s}{\partial z} + \frac{\partial W}{\partial s} + \frac{\partial \overline{V}}{\partial z} = \frac{q^*}{Gt} \qquad (17)$$

Compatibility condition,

$$\oint \frac{\partial W}{\partial s} \, ds = 0$$

must be also satisfied.

We obtain

$$q^* = G(\theta_s' + \bar{\theta}') \frac{2F}{\oint \dfrac{ds}{t}} \qquad (18)$$

We get primary torsional moment m_t by performing integration of $q^* r_D$

$$m_t = \oint q^* r_D = G(\theta'_s + \bar{\theta}') I_B \qquad (19)$$

where

$$I_B = \frac{4F^2}{\oint \dfrac{ds}{t}} \qquad (20)$$

Secondary torsional moment $\bar{m}_t$ is as follows

$$\bar{m}_t = \int_F \bar{q} r_D ds \qquad (21)$$

From the Eq. (13)

$$\int_F \bar{q} \frac{F^*}{t} ds = 0 \qquad (22)$$

where

$$F^* = \frac{2F}{\oint \dfrac{ds}{t}}$$

The Eq. (21) is therefore equal to

$$\bar{m}_t = -E\theta'''_s \int_F (F_\varphi - \bar{q}_x)\left(r_D - \frac{F^*}{t}\right) ds \qquad (23)$$

Substituting the relation $\oint \bar{q}_x(r_D - F^*/t) \, ds = 0$ into the above equation, then integrating this by part, and we obtain

$$\bar{m}_t = -E\theta'''_s \left[F_\varphi \int \left(r_D - \frac{F^*}{t}\right) ds\right] + E\theta'''_s \int_F \varphi t(\varphi_0 - \varphi) \, ds$$

The first term of the right side vanishes, we find

$$\bar{m}_t = -E\theta'''_s \int_F \varphi^2 \, dF = -E\theta'''_s C_w \qquad (24)$$

where

$$C_w = \int_F \varphi^2 \, dF$$

The torsion costant I_t is given as follows

$$I_t = I_s + I_B \qquad (25)$$

Total torsional moment T is obtained as follows

$$T = m_t + \bar{m}_t = GI_t(\theta'_s + \bar{\theta}') - EC_w \theta'''_s \qquad (26)$$

Calculation of shear center D can be made in the same manner as the torsion-bending theory.

$$y_D = \frac{\int_F \varphi x \, dF}{\int_F x^2 \, dF}, \qquad x_D = \frac{\int_F \varphi y \, dF}{\int_F y^2 \, dF}$$

4. Determination of Additional unit Rotation

Zero points of the secondary shear flow are denoted by S_1, S_2, S_3 $\cdots$, as shown in Fig. 6.

Secondary torsional moment is divided into two parts, One is a positive part of $\bar{q}$ and the other is a negative part of $\bar{q}$, We obtain
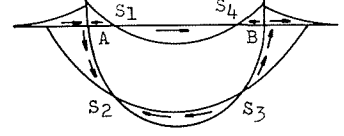

Fig. 6. Secondary shear flow $\bar{q}$

$$\overline{m}_t = \int_{(+)} \bar{q} r_D ds + \int_{(-)} \bar{q} r_D ds = \overline{m}_{t1} + \overline{m}_{t2} \tag{27}$$

We define that the angle of rotation corresponding to $\overline{m}_{t1}$ and $\overline{m}_{t2}$ are $\bar{\theta}_1$ and $\bar{\theta}_2$ respectively.

The internal work by $\overline{m}_{t1}$ and $\overline{m}_{t2}$ are $\overline{m}_{t1}\bar{\theta}_1'$ and $\overline{m}_{t2}\bar{\theta}_2'$ and internal work are as follows correspondingly

$$\frac{1}{G} \int_{(+)} \frac{\bar{q}^2}{t} ds, \qquad \frac{1}{G} \int_{(-)} \frac{\bar{q}^2}{t} ds$$

The external work must be equal to the internal work, we obtain

$$\left. \begin{aligned} \bar{\theta}_1' &= -\frac{E\theta_s'''}{G\varPhi_1} \int_{(+)} \frac{\bar{q}_1^2}{t} ds \\ \bar{\theta}_2' &= -\frac{E\theta_s'''}{G\varPhi_2} \int_{(-)} \frac{\bar{q}_2^2}{t} ds \end{aligned} \right\} \tag{28}$$

where

$$\bar{q}_1 = -\frac{\bar{q}_{(+)}}{E\theta_s'''}, \qquad \bar{q}_2 = \frac{\bar{q}_{(-)}}{E\theta_s'''}$$

$$\varPhi_1 = \int_{(+)} \bar{q}_1 r_D ds, \qquad \varPhi_2 = \int_{(-)} \bar{q}_2 r_D ds$$

Symbols of $(+)$ and $(-)$ represent a positive and a negative part of $\bar{q}$ respectively. The resultant unit rotation due to $\bar{\theta}_1'$ and $\bar{\theta}_2'$ is denoted by $\bar{\theta}'$.

Additional angle yieding by the unit rotation $\bar{\theta}_1'$ and $\bar{\theta}_2'$

$$\bar{\theta}' = \bar{\theta}_1' + \bar{\theta}_2' \tag{29}$$

by the reciprocal law we obtain

$$\overline{m}_{t1}\bar{\theta}_2' - \overline{m}_{t2}\bar{\theta}_1' = 0$$

we find

$$\bar{\theta}' = -\frac{E}{G} \frac{1}{\varPhi_1 + \varPhi_2} \left(\int_{(+)} \frac{\bar{q}_1^2}{t} - \int_{(-)} \frac{\bar{q}_2^2}{t} ds \right) = -\alpha_0 \theta_s''' \tag{30}$$

where

$$\alpha_0 = \frac{E}{G} \frac{1}{\varPhi_1 + \varPhi_2} \left(\int_{(+)} \frac{\bar{q}_1^2}{t} ds - \int_{(-)} \frac{\bar{\theta}_2^2}{t} ds \right) \tag{31}$$

Substituting this in Eq. (26). We obtain the following fundamental differential equation for torsion-bending.

$$GI_t\theta_s' - E\bar{C}_w\theta_s''' = T \tag{32}$$

where

$$\alpha = \alpha_0 \frac{GI_t}{EC_w}, \qquad \bar{C}_w = C_w(1+\alpha) \tag{33}$$

In case of a box cross section with constant thickness the coefficient is reduced to

$$\alpha = \frac{0.4\{(1+\beta)(1+4\beta+\beta^2)/2 - 2\sqrt{3}/9(1+2\beta)^{2.5}\}\{1+1/3 \cdot t^2/h^2(1+\beta^2)\}}{(1-\beta^2)\{(1-\beta)/2 + \sqrt{3}/9(1+2\beta)^{1.5}\}} \tag{34}$$

where

$$\beta = h/b$$

The coefficient α has a limit value where the cross section is square.

$$\lim_{\beta \to 1} \alpha = 0.4(1 + 4/3 \cdot t^2/h^2) \tag{35}$$

The values of coefficient α calculated by Eq. (33) in the case of $\gamma = 1.0$, $F = 9$ m^2 are shown in Fig. 7 and compared with Grasse's. Fig. 8 shows the values of α in the case of different thicknesses, when the area of cross section is constant.
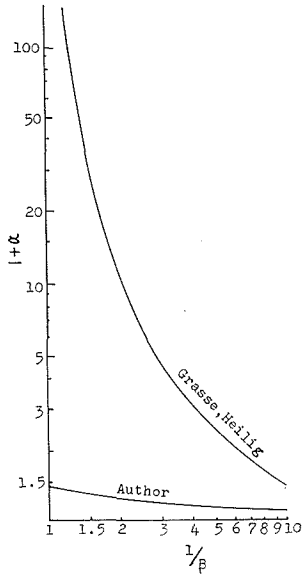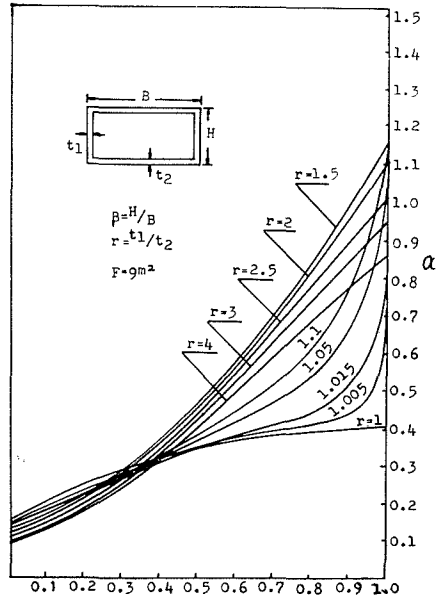

Fig. 7.

Fig. 8.

5. Model beam test

In order to ascertain the theory of torsion-bending in consideration of the secondary deformation, a model beam is tested and the strain yielded by the warping moment is measured by a electric strain gauge. A maximum strain occurs locally at the warped point and loading point, thus the strain is measured at the fixed end of the cantilever.

5.1 Test procedure

The material is acrylic resin and the dimension of the box beam is 50 cm in length, 4 cm in width and 3 cm in height and details of the cross section are shown in Fig. 9. The fixed end is hardened by bolts. As the material is sensitive to temperature, the test is performend in a constant temperature room (19.5°C).

The Modulus of elasticity and shear modulus are determined by deformation due to vertical load and torsional load as shown in Fig. 9.

$$E = 36600 \text{ kg/cm}^2$$

$$G = 14400 \text{ kg/cm}^2$$

5.2 Test results

In Fig. 10 the strain given by this test is compared with the strain theoretically given by Bornscheuer, Grasse and the author. The values have a variation of about $\pm 10 \times 10^{-6}$ due to the influences of temperature and vibration by loading, but this value falls between Bornscheuer's and Grasse's values and corresponds well with the author's, therefore it is clear that the theory is more exact than anothers.

6. Analysis of continuous beam with variable cross section

Fig. 9. Deformation

Fig. 10. Test results

A simple beam with a torsional load is assumed to have a statically determinate principal system and the internal forces of a continuous beam are analyzed by determination of redundant forces at the end of a simple beam.

6.1 Principal system

The moment of a beam with variable cross sections are given by the "Knoten Last" method[9]. We define the notation m as follows.

$$m = GI_t\theta'_s \tag{36}$$

Substituting this into Eq. (32), we obtain

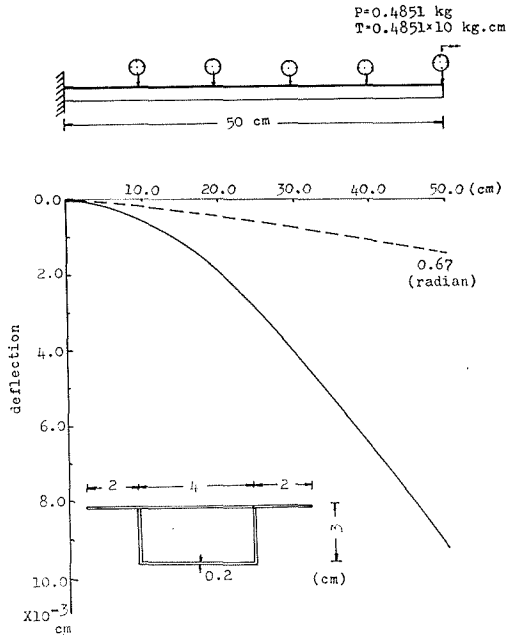$$m'' - \bar{\lambda}^2 m + \bar{\lambda}^2 T = 0 \tag{37}$$

where
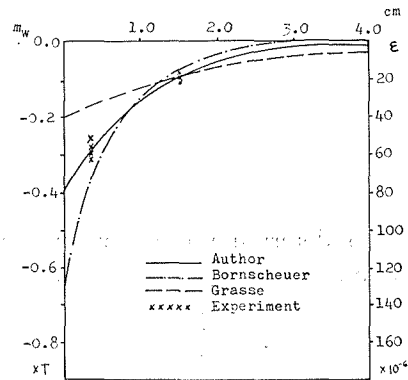
$$\bar{\lambda} = \sqrt{GI_t/E\bar{C}_w}$$

We assume that the distribution of torsional moment m has a parabolic form and we divide a beam into $(n+1)$ part and each part is applied to Eq. (37).

We find

$$-m_{n-1}(1-r_{n-1}) + m_n(2+10\,r_n) - m_{n+1}(1-r_{n+1}) = \varDelta z K_n(\bar{\lambda}^2 T) \qquad (38)$$

where

$$r = \bar{\lambda}^2 \varDelta z^2/12, \qquad \varDelta z = l/n+1$$

We can denote the Eg. (38) in a matrix form.

$$\begin{bmatrix} -(r-r_0) & (2+10\,r_1) & -(1-r_2) & & & 0 \\ 0 & -(1-r_1) & (2+10\,r_2) & -(1-r_3) & & \\ \vdots & & \ddots & \ddots & \ddots & \\ 0 & & -(1-r_{n+1}) & (2+10\,r_n) & -(1-r_{n+1}) \end{bmatrix} \begin{bmatrix} m_0 \\ \vdots \\ \vdots \\ m_{n+1} \end{bmatrix} = \begin{bmatrix} \varDelta z K_1(\bar{\lambda}^2 T) \\ \varDelta z K_2(\bar{\lambda}^2 T) \\ \vdots \\ \varDelta z K_n(\bar{\lambda}^2 T) \end{bmatrix}$$

$$(39)$$

The number of equations is n and that of the unknown is $(n+2)$, therefore two boundary conditions are necessary. Boundary conditions of simple beams are as follows

$$m_0' = m_{n+1}' = 0 \qquad (40)$$

we transform by the Knoten Last method

$$(1+5\,r_0)\,m_0 - (1-r_1)\,m_1 = \varDelta z K_0(\bar{\lambda}^2 T) \qquad (41)$$

$$(1-r_n)\,m_n - (1+5\,r_{n+1})\,m_{n+1} = \varDelta z K_{n+1}(\bar{\lambda}^2 T) \qquad (42)$$

In order to determine the distribution of total moment T, a beam is subjected to $T=1$ as shown in Fig. 11, then the right side of the Eq. (38) becomes

$$\varDelta z K_0(\bar{\lambda}^2 T) = 0.5\,(7\,r_0 + 6\,r_1 - r_2)$$
$$\varDelta z K_i(\bar{\lambda}^2 T) = r_{i-1} + 10\,r_i + r_{i+1} \qquad (43)$$
$$\varDelta z K_j(\bar{\lambda}^2 T) = 0.5\,(-r_{j-2} + 6\,r_{j-1} + 7\,r_j)$$
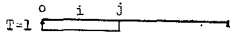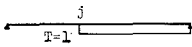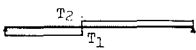
Fig. 11.

Fig. 12.

Fig. 13.

Where i represents an arbitrary point considered and j is the point which is subjected to a concentrated load. Eq. (41) can also be applied to the case of Fig. 12. and then the solution of Eq. (38) in the both cases as shown in Fig. 11 and 12 are called m_L and m_R respectively. The total torsional moments are denoted by T_1 and T_2 as shown in Fig. 13.

To satisfy condition that angle of rotation must be zero on the both ends of the beam.
we obtain

$$T_1 \int_0^l \frac{m_L}{GI_t}\,dz + T_2 \int_0^l \frac{m_R}{GI_t}\,dz = 0 \qquad (44)$$

we find

$$T_2 = -\int_0^l \frac{m_L}{GI_t}\, dz \bigg/ \int_0^l \frac{m_{T=1}}{GI_t}\, dz \tag{45}$$

where $m_{T=1}$ corresponds to the case of loading $T=1$ over the beam.

Substituting the Eq. (45) into the right side of Eq. (38), we obtain the solution by matrix-analysis.
From Eq. (32) we find

$$m'' = \bar{\lambda}^2(m-T)$$

and primary torsional moment is

$$m_t = m - \alpha_0 m'' \tag{46}$$

secondary torsional moment $\bar{m}_t$ becomes

$$\bar{m}_t = T - m_t \tag{47}$$

we difine the warping moment m_w as follows

$$m_w = -EC_w \theta_s'' \tag{48}$$

we obtain from Eq. (32)

$$m_w - \bar{\lambda}^2 m_w = 0 \tag{49}$$

The slope of warping moment is discontinuous at the point of concentrated load, therefore an additional load, m_w' left $-m_w$ right, must be considered.
we assume that m_w is of a parabolic form and transform Eq. (49) in a matrix form.

$$\begin{bmatrix} -(1-r_0) & (2+10\,r_1) & -(1-r_2) & & 0 \\ & & & & \\ 0 & & (1-r_{n-1}) & (2+10\,r_n) & -(1-r_{n-1}) \end{bmatrix} \begin{bmatrix} m_{w0} \\ \vdots \\ \\ \vdots \\ m_{w\,n+1} \end{bmatrix} = \begin{bmatrix} 0 \\ \\ \dfrac{1+r_j}{1+\alpha_j} \\ \\ 0 \end{bmatrix} \tag{50}$$

where j represents the point of load the two boundary conditions of a simple beam are as follows

$$m_{w0} = m_{w\,n+1} = 0 \tag{51}$$
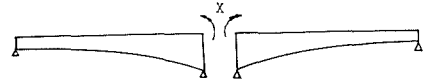

Fig. 14. Redundant warping moment

6.2 Analysis of cotinuous beam

Two boundary conditions are necessary in the case of acting a redundant warping moment as shown in Fig. 14.

$$(1+5\,r_0)\,m_0 - (1-r_1)\,m_1 = 0$$
$$-0.5\,r_{n-1}\,m_{n-1} - (1-3\,r_n)\,m_n + (1+3.5\,r_{n+1})\,m_{n+1} = -\varDelta z\,GI_{t\,n+1}/EC_{w\,n+1} \tag{52}$$

Substituting this into matrix (38)

$$
\begin{bmatrix}
(1+5r_0) & -(1-r_1) & 0 & & & \\
-(1-r_0) & (2+10r_1) & -(1-r_2) & & & \\
& & & & & \\
& & -(1-r_{n-1}) & (2+10r_n) & -(1-r_n) \\
& & -0.5r_{n-1} & -(1-3r_n) & (1+3.5r_{n+1})
\end{bmatrix}
\begin{bmatrix} m_0 \\ \vdots \\ \vdots \\ \vdots \\ m_{n+1} \end{bmatrix}
=
\begin{bmatrix} 0 \\ \vdots \\ \vdots \\ \vdots \\ -\Delta z \dfrac{GI_{t\,n+1}}{EC_{w\,n+1}} \end{bmatrix}
\tag{53}
$$

denoting above solution of m_{n+1} on the first span by m^1_{n+1}, similar to the case of second span by m^2_{n+1} and the solution of m_{n+1} in the case of simply supported beam by δ^j_{10}, we get a redundant force.

$$
X^j_1 = \frac{-\delta^j_{10}}{m^1_{n+1} + m^2_{n+1}}
\tag{54}
$$

Influence lines of internal moment can be calculated,

$$
S = S_0 + \sum S_x X
\tag{55}
$$

S_0 corresponds to the influence line of a simple beam, in the case of calculating for m_t, internal force S_x can be obtained from Eq. (48) and in case of m_w. we obtain as follows

$$
\begin{bmatrix}
(2+10r_1) & -(1-r_2) & 0 & & & & 0 \\
-(1-r_1) & (2+10r_2) & -(1-r_3) & & & & \\
& & & & & & \\
& & & -(1-r_{n-2}) & (2+10r_{n-1}) & -(1-r_n) \\
& & & & -(1-r_{n-1}) & (2+10r_n)
\end{bmatrix}
\begin{bmatrix} m_{w1} \\ \vdots \\ \vdots \\ \vdots \\ m_{w\,n} \end{bmatrix}
=
\begin{bmatrix} 0 \\ \vdots \\ \vdots \\ 0 \\ 1-r_{n+1} \end{bmatrix}
\tag{56}
$$

7. Numerical example

The general view of the continuous girder bridge with three spans is shown in Fig. 15. As the greatest difference between the author's theory and theories of other workers appears at an intermediate support, then the comparison may be shown only at this point. The condition of loading is determined to result in maximum shearing stress. The line load of 5 t/m and uniform load of 0.35 t/m² are applied as

Fig. 15. General view (case 1)

Table 2.

	L m	I_t m⁴		C_w m⁶		α	
		1	2	1	2	1	2
Case 1	40	1.56	10.6	1.02	3.75	0.16	0.48
Case 2	50	1.72	13.4	1.14	4.23	0.17	0.51
Case 8	60	2.67	16.4	1.56	4.06	0.23	0.51

P=5^t/m
p=0.35^t/m^2

Fig. 16. Live load

------ Author
--·--·-- Bornscheuer
-------- simple torsion

Fig. 17. Influence line of m_t (at point 2)

Fig. 18. Influence line of $\overline{m}_t$ (at point 2)
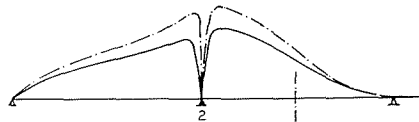
Fig. 19. Influence line of m_w (at point 2)

Case 1   kg/cm^2

2.3
4.3
7.0

Case 2

2.3
4.4
6.3

Case 3

2.3
4.5
5.8

-------- simple torsion
--·--·-- Bornscheuer
------ Author
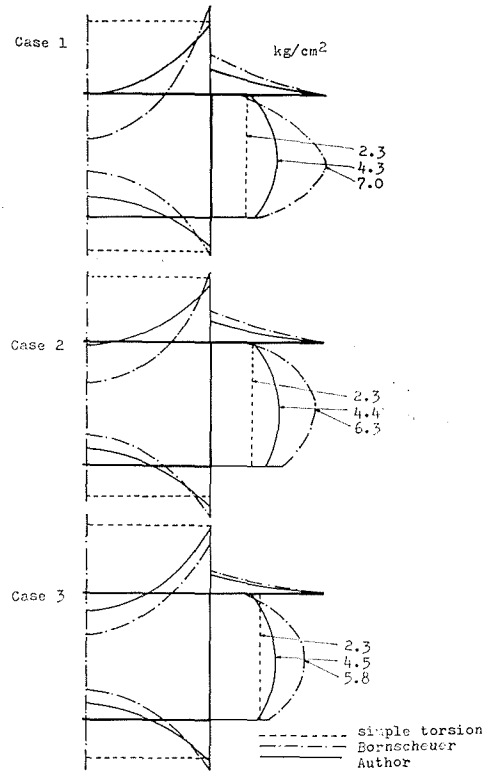
Fig. 20. Resultant shearing stress

shown in Fig. 16. Fig. 17, Fig. 18 and Fig. 19 show influence lines of m_t, $\overline{m}_t$ and m_w in a comparison of the theories. Distributions of the shearing stresses on the continuous beam having a different span are shown in Fig. 20.

8. Conclusion

The following conclusions have been drawn

(1) With regard to the magnitude of the coefficient α indicating the effect of the deformation of secondary shearing stress, there is a large differece between the author's theory and Grasse's. The coefficient derived by Grasse is so large that the warping resistance C_w is negligible, but in the author's theory, the maximum value is in practice from 0.4 to 1.5.

(2) With regard to test results, it is ascertained that the proposed thory is more exact than Bornscheuer's and Grasse's.

(3) As to influence lines, there is some difference between the present theory and other's on the simply supported end, but large differences appear at the intermediate support. The influence lines by the proposed theory take an intermediate

value between Bornscheuer's and simple torsion theory.

(2) Resultant shearing stresses calculated by this theory for a continuous concrete girder bridge are in practice from 20% to 40% less than those by Bornscheuer, and two times more than those of simple torsion.

Reference

1) Noboru Saeki: Warping torsion theory in consideration of the deformation due to secondary shearing stress and its numerical examples. Proceedings of the Japan society of civil engineers, No 209.

2) Wagner, H.: Luftfahrt-Forschung Band 11. 1939, S. 119.

3) Bornscheuer, F. W.: Systematishe Darstellung des Biege und Verdrehvorgangs unter besonderer Berücksichtigung der Wölbkrafttorsion, Stahlbau 21-1.

4) Vlasov, V. Z.: Thin-Walled Elastic Beams.

5) Heilig, R.: Beitrag zur Theorie der Kastenträger beliebiger Querschnittsform, Stallbau 11/1961.

6) Roik, K. und Sedlacek, G.: Theorie der Wölbkrafttrsion unter Brücksichtigung der sekundären Schubverformungen Analogiebetrachtung zur Berechnung des quer belasten Zugstabes, Stahlbau 2/1966.

7) Grasse, W.: Wölbkrafttorsion dünwandiger prismatischer Stabe beliebigen Querschnitts, Ingnieur-Archiv, XXXIV. Band, 1965.

8) Timoshenko and Goodier, Theory of Elasticity, S. 284.

9) Stüssi, Futz: Entwurf und Berechnung von Stahlbauten.